



ISSN: 2723-9535



Available online at www.HighTechJournal.org

HighTech and Innovation Journal

Vol. 3, No. 4, December, 2022



Punching Shear Characterization of Steel Fiber-Reinforced Concrete Flat Slabs

Abbas H. Mohammed ^{1*}, Huda M. Mubarak ¹, Ali K. Hussein ²,
Taymour Z. Abulghafour ², Dia Eddin Nassani ³

¹ Civil Engineering Department, University of Diyala, Diyala, 32001, Iraq.

² Civil Engineering Department, Bilad Alrafidain University College, Diyala, 32001, Iraq.

³ Civil Engineering Department, Hasan Kalyoncu University, Gaziantep, 27500, Turkey.

Received 12 September 2022; Revised 10 November 2022; Accepted 17 November 2022; Published 01 December 2022

Abstract

Punching shear failure in thin slabs under concentrated loads can cause shear stresses near columns. The use of steel fiber is a practical way to improve a slab-column connection's punching strength and deformation capacity. In this study, the capacity and behavior of steel fiber-reinforced concrete flat slabs are examined under punching shear force. Ten small-scale flat slabs were tested, eight of which had steel fiber and two without. Two parameters are studied in this paper, which are the fiber volume ratio (from 0% to 2%) and the stub column load shape (circle and square). The test results include the concrete compressive strength, crack patterns, punching shear, and load-deflection behavior of the slabs. Based on the experimental results, it was found that the punching shear capacity of slabs with steel fiber (S5) increased by 21.8% compared to slabs without steel fiber (S1), and the slabs with steel fiber had more ductility compared to the slabs without fiber.

Keywords: Flat Slab; Steel Fiber Reinforced Concrete; Crack; Punching Shear Resistance; Concrete Structures.

1. Introduction

Reinforced concrete (RC) flat slabs are often utilized in the construction of medium-rise commercial buildings, residential structures, and parking garages due to the advantages that they provide in terms of both construction and aesthetics. The flat slab requires less formwork and reinforcement, which simplifies placement and installation and enables shorter total story heights. It is common for the punched shear capacity at the slab-column connections in RC flat slabs to be the determining factor in the ultimate strength of slab. This failure process is often sensitive, which results in gradual collapses that eventually lead to the destruction of the whole structure [1–3]. There are a few different approaches that may be undertaken in order to increase the capacity of punching shear, including the use of bent-up bars, closed stirrups, post-installed shear reinforcement and shear studs. Recent research [4–9] has been performed to examine the viability of using Fiber-Reinforced Concrete (FRC) to increase punching shear capacity. According to the findings of these experiments, the punched shear strength as well as the deformational capacity of FRC slabs have increased. The bridging activity of the fibers, which happens after the cracking of the concrete matrix, is primarily responsible for this phenomenon.

* Corresponding author: abbas_mohammed_eng@uodiyala.edu.iq

 <http://dx.doi.org/10.28991/HIJ-2022-03-04-08>

➤ This is an open access article under the CC-BY license (<https://creativecommons.org/licenses/by/4.0/>).

© Authors retain all copyrights.

Numerous theoretical and experimental studies have already examined the positive impacts of steel fibers on punching shear resistance [10–15]. Steel fibers fill in shear cracks in concrete, which improves the material's ability to soften under tension and, as a result, the overall deformational influence. Steel fibers, based on fiber type and characteristics, may also contribute significantly to punching resistance [17–18]. The current slab-column connection code provisions, such as ACI 318-11 [19], Fib Model Code 2010 [20, 21], and JSCE 2007 [22], were developed for normal concrete structures. In the case of FRC slab-column connections, their application is not always a simple process, especially for empirical design equations. Several different specialized models for the punching shear of FRC slab-column connections had been suggested over the course of the past several decades. A punching shear capacity design equation for a Steel Fiber Reinforced Concrete (SFRC) slab was developed by Narayanan & Darwish [5]. This equation considers compressive zone strength above inclined fractures, fiber pull-out shear forces, and dowel and membrane shear forces.

An empirical design formula for SFRC slab-column connections was developed by Harajli et al. [7], using linear regression as the primary statistical method. This equation was developed empirically. Truong et al. [23] developed an equation for the design process that was based on the SFRC failure criteria. This equation was the result of a theoretical investigation that they carried out. The formula that has been suggested takes into consideration both thin slabs that have high span-to-thickness ratios as well as the assumption that tensile reinforcement will fail before punched shear failures. At the critical section, both the compressive and tensile zones were taken into consideration. Furthermore, It was thought that tensile cracking, rather than compressive crushing, had been responsible for determining the capacity of punching shear. The design equation for estimating the capacity of punched shear of standard concrete slab-column connections has been recently developed by Higashiyama et al. [24]. This equation is based on the JSCE model and was developed very recently.

In this paper an experimental study of the impact of steel fiber on the cracking behavior and the punching shear capacity and of SFRC slabs. Ten small-scale flat slabs with different fiber volume percentages were investigated.

2. Experimental Program

2.1. Test Setup and Procedure

To evaluate the impact of steel fibers for reinforcing of concrete elements, punching shear and compressive strength tests were performed on slab specimens and cubes. Table 1 provides information on the concrete cubes' 7, 14, and 28-day compressive strengths.

Table 1. Compressive strength of cubes

	Reinforced concrete without fiber (MPa)	SFRC (MPa)
7 Days	36.8	38.9
7 Days	38.7	39.7
14 Days	45.4	46.1
14 Days	46.9	47
28 Days	48.8	58.2
28 Days	49.2	59.8

A linear variable differential transducer (LVDT) with a 25 mm stroke was utilized to calculate mid-span deflections, as displayed in Figure 1. The load, actuator, and LVDT values were captured by the collecting data system in the center of the specimen. At a deflection rate of 0.25 mm/min, a displacement control scenario test system was employed to execute the trials.

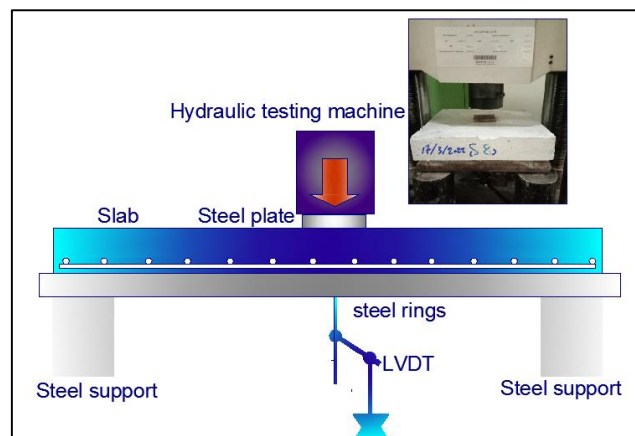


Figure 1. Test arrangement

The loads are applied through a circular and rectangular steel column stub. It was positioned in the center of the slab being tested and was used to simulate the inner column. After applying load to the column stub, the support system evenly distributed the weight on the slabs along the steel ring edge. Every specimen was loaded past its maximum capacity in order to observe the slab's behavior following punching. Once the column stub had inserted itself 55 mm into the specimen, the tests were declared complete. Throughout the test, deflections and loads were continually monitored as well as recorded using an automated data acquisition system.

2.2. Specimen Preparation

To verify the mechanical characteristics of the slabs, the slab specimens were made from the same concrete mix.. A 150 mm cube served as the basis for the prototype casting. Ten identical slab specimens were cast, as shown in Table 2. Each steel fiber ratio was represented by two identical slab specimens. The first one was utilized for testing by a square column, and the second was utilized for testing by a circle column. In order to get the dimensions of the slabs, prototype slabs were scaled down by a ratio of one-third, and they were similar in shape and size. The slabs dimensions were 45×45×8 cm. Figure 2 shows the dimensions of the tested slabs.

Table 2. Specimen designation

Sample Designation	Type of Column	Steel Fiber Ratio
S1	Square	0.0%
S2	Square	0.5%
S3	Square	1.0%
S4	Square	1.5%
S5	Square	2.0%
S6	Circle	0.0%
S7	Circle	0.5%
S8	Circle	1.0%
S9	Circle	1.5%
S10	Circle	2.0%

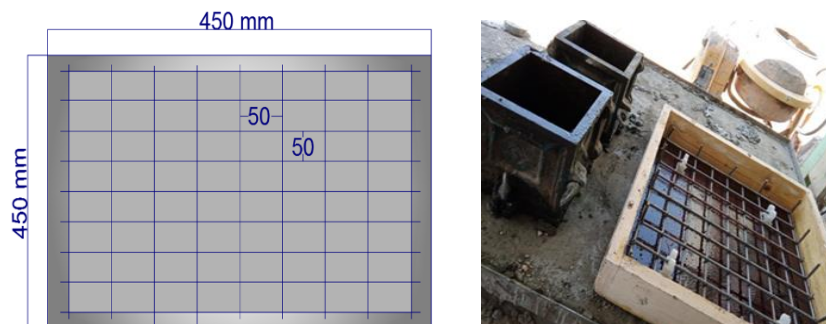


Figure 2. Dimension of test slabs

The dimensions of the square and circle stub columns are (100×100) mm and (100) mm, respectively. The (ASTM C 143/C143M-15a) slump experiment was used to evaluate the fresh-state behavior of all mixtures, whether they contained fibers or not. Following the slump test, the test slabs and control specimens were cast immediately. Polythene sheets were placed on top of all slabs and cubes to prevent moisture from evaporating on the first day following casting. After 24 hours, the cube and slab formwork were removed from their molds. The curing temperature for all specimens, both in water and in air, was about 23.5 °C, according to ASTM C 1064/C1064M-12.

3. Results and Discussion

3.1. Cracking Patterns

Figure 3 summarizes the cracking characteristics of all test specimens. The RC specimens failed abruptly and brittlely with the development of a single crack. All test specimens that contained fibers showed several microcracks as well as one distinct localized crack. Crack localization is the term for this phenomenon, as seen in Figure 4. The S5 slab had the optimum cracking qualities in terms of crack spacing and number of cracks. The S5 slab also has the optimum post-cracking flexural characteristics involving high flexural strength, toughness values, and ductility. A significant reduction in average fracture width of about 42% was seen when S5 was compared to S1.



Figure 3. Slabs after test



(a) Slab S9

(b) Slab S6

Figure 4. Crack pattern

The slabs with steel fiber were shown to have more microcracks because of their stiffer post-cracking behavior. Due to its greater stiffness, the crack's extension was effectively resisted, which caused further steady-state flat and microcrack cracks to form following the initial cracking. From these findings, it's significant that the cracking characteristics are powerfully affected by the properties in the hardening region (i.e., post-cracking stiffness, deflection capacity, and strength).

3.2. Load-Displacement Curve

The load-displacement curves are displayed in Figures 5 to 7. All SFRC slabs had linear load-deflection responses up until the onset of the first flexural fracture during the initial phases of loading. Up to this moment, once the flexural stress there is equal to the composite material's cracking stress, the slab is considered to be in an elastic condition. Elastic behavior is displayed in the composite material in both compression and tension, and there were no cracks in the specimens. Strain and stress are reportedly directly related to slab thickness. The first cracks to occur at the tension face of the slab are radial fractures that stretch from the column face to the slab border. When increasing the load, the several of cracks and their breadth increased until failure.

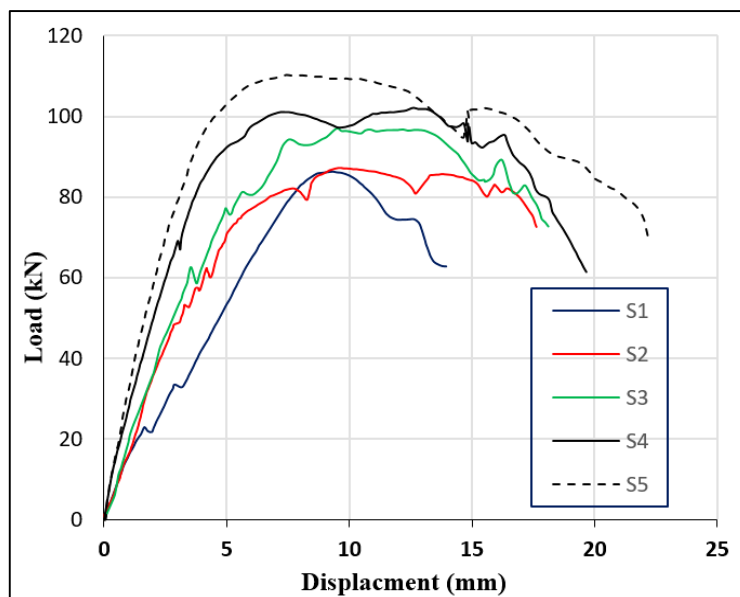


Figure 5. Load - central deflection for slabs without steel fiber

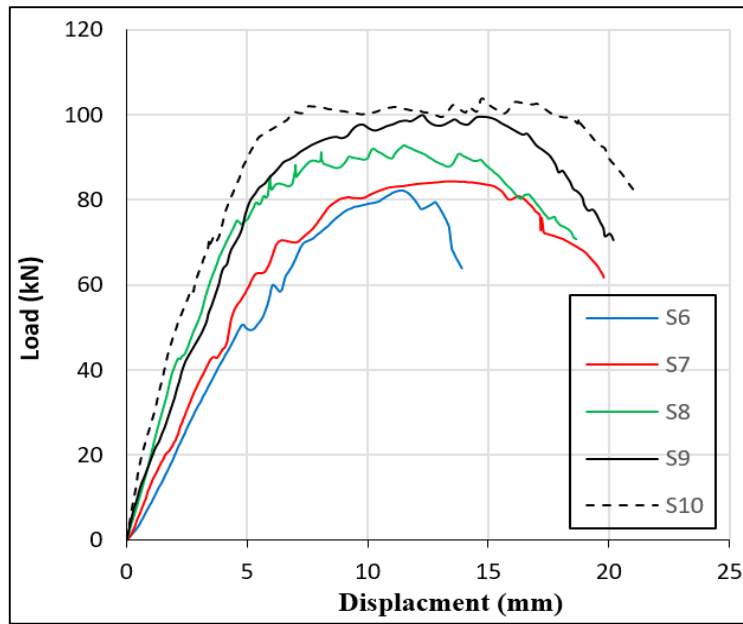


Figure 6. Load - central deflection for slabs with steel fiber

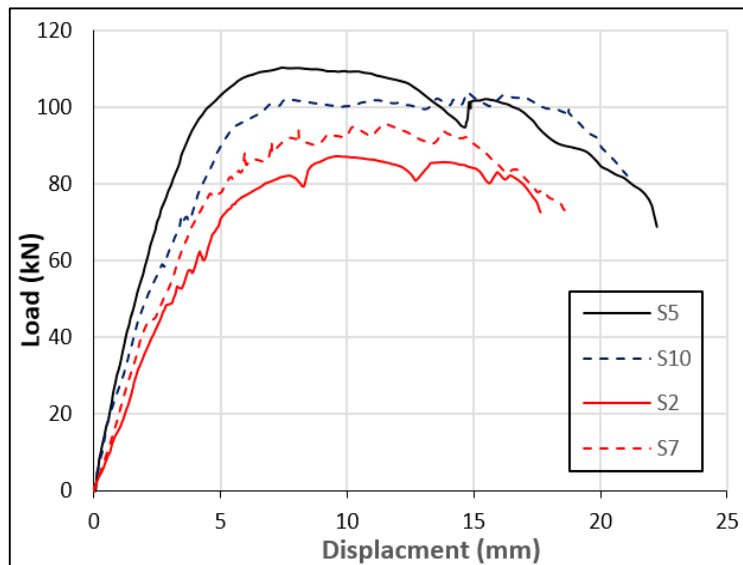


Figure 7. Effect of steel fiber and column shape

The flexural fracture or hinge develops as a result of a sudden decline in the slab's capacity to support loads, as can be seen in the load-deflection charts. The flexural crack caused the slab's bending resistance to drop in an orthogonal direction. For the slabs without steel fiber, the failure was abrupt, brittle, and accompanied by rather wide fracture widths and spalling (Figure 4b). This is a result of the reality that basic concrete material has lower toughness, lower tensile strength, lower shear strength, lower flexural strength, as well as brittle character. A flexural crack or hinge forms in such slabs when the loading capacity of the slab suddenly decreases, as seen in Figures 5 to 7.

As illustrated in Figure 5, the slab's bending resistance decreased significantly in the opposite direction of the flexural crack, and the slabs without fibers showed a significant decrease in rigidity. For slab S1, the deflection at the ultimate load was 13.9 mm, while for slab S5, it was 22.2 mm. Slabs S5 and S10 had maximum deflections of 22.2 and 21 mm, respectively, under the ultimate load. The ultimate deflection for slabs S5, S4, S3, and S2 increased by 42%, 34%, 29%, and 27%, respectively, compared to slab S1.

3.3. Punching Shear

Table 3 shows the peak load for the slabs. Figures 5 to 7 show the load levels at which deformation occurred. The ultimate capacity is affected by the fibers utilized. The ultimate load increased by 21.3% in the S5 slab with a fiber volume percentage of 2% as compared to the S1 slab. When the SFRC slab cracks, the tensile stress is transmitted to the steel fibers that bridge the crack length, whereas the slab's uncracked portion retains its tensile strength. As a result of

the crack spreading towards the slab's compression face, the neutral axis will move. Due to these tensile stress processes in the tension zone and the gradual displacement of the slab section's neutral axis, The load-deflection relationship curve has a flattening ascending form. This indicated that the steel fibers applied to RC slabs increased structural strength. Additionally, the advantage of the fibers was immediately apparent in the slab's ultimate strength, featuring a decreased loss in load-bearing capability with each step of cracking. Moreover, another indication of steel fiber in the slab was its toughness, which was related to the area under the load- displacement curve (Figures 5 to 7).

Table 3. Peak loads of the tested slabs

Sample Designation	Type of Column	Peak Loads (kN)
S1	Square	85.6
S2	Square	87.1
S3	Square	96.45
S4	Square	102.5
S5	Square	110.3
S6	Circle	81.6
S7	Circle	84.3
S8	Circle	92.7
S9	Circle	100.1
S10	Circle	103.7

The failures are more gradual in the S5 and S10 slabs. Furthermore, increasing the fiber content causes the fibers to be distributed more evenly and densely throughout the concrete, which lowers shrinkage cracks and enhances post-crack strength. Numerous tests also supported this, which found that employing mixtures of steel fibers and polypropylene fibers resulted in improved post-peak residual strength responses [25, 26]. The experimental results showed that utilizing steel fibers improved the ductile conductivity and caused more deformations on the compression side, enhancing the deformability and punching shear capacity. However, in the S5 and S10 slabs, the deformability values enhanced punching shear resistance considerably. This is a result of the capability of steel fibers to bridge smaller micro-cracks, which improves flexural properties in comparison to individual steel fibers. Figure 7 shows that the square column (S5) is 11% more effective in terms of capacity for punching shear compared to the circle column (S10). This is due to the fact that the area of the square column (100 mm^2) is greater than the area of the circular column (78.5 mm^2), which in turn causes the stress of the circular column to be greater than the stress of the square column.

4. Conclusion

In this paper, an experimental program was presented to study the effect of steel fiber content (from 0% to 2%) and the stub column load shape on the behavior of the slab. The load-displacement behavior, punching shear, and crack patterns of the slabs were all measured and reported on in the tests. According to the experimental findings, it was noted that the punching shear capacity of slabs with steel fiber (S5) increased by 21.8% compared to slabs without steel fiber (S1). The slabs with steel fiber have a significant ductile behavior, and their contribution to energy absorption of slab was improved the ductility more than none RC. Additionally, radial cracks extend from column to slab border, and the first cracks appear at the slab tension face. The several of cracks and their width increased until failure when the load increased.

The findings reported in this study demonstrated that the square column is more effective than the circular column in terms of punching shear capability. This is because the area of the square column (100 mm^2) is greater than the area of the circle column (78.5 mm^2), which leads to the fact that the stress of the square column is less than the stress of the circle column. When compared to equivalent slabs without steel fibers, concrete specimens containing steel fibers may exhibit dramatically improved deformation behavior. Additionally, the advantage of the fibers was immediately apparent in the slab's ultimate strength, featuring a decreased loss in load-bearing capability with each step of cracking. In addition, another indicator of steel fiber was its toughness, which was connected to the area under the load- displacement curve.

5. Declarations

5.1. Author Contributions

Conceptualization, A.H.M. and A.K.H.; methodology, A.H.M.; software, H.M.M.; validation, A.H.M., A.K.H., and H.M.M.; formal analysis, H.M.M.; investigation, A.H.M.; resources, T.Z.A.; data curation, A.K.H.; writing—original draft preparation, A.K.H.; writing—review and editing, D.E.N.; visualization, H.M.M.; supervision, D.E.N.; project administration, T.Z.A.; funding acquisition, H.M.M. All authors have read and agreed to the published version of the manuscript.

5.2. Data Availability Statement

The data presented in this study are available in the article.

5.3. Funding

The authors received no financial support for the research, authorship, and/or publication of this article.

5.4. Declaration of Competing Interest

The authors declare that they have no known competing financial interests or personal relationships that could have appeared to influence the work reported in this paper.

6. References

- [1] Schousboe, I. (1976). Bailey's Crossroads Collapse Reviewed. *Journal of the Construction Division*, 102(2), 365–378. doi:10.1061/jcceaz.0000612.
- [2] Kaminetzky, D., & Carper, K. L. (1992). Design and construction failures: Lessons from forensic investigations. *Journal of Performance of Constructed Facilities*, 6(1), 71–72. doi:10.1061/(asce)0887-3828(1992)6:1(71).
- [3] King, S., & Delatte, N. J. (2004). Collapse of 2000 Commonwealth Avenue: Punching Shear Case Study. *Journal of Performance of Constructed Facilities*, 18(1), 54–61. doi:10.1061/(asce)0887-3828(2004)18:1(54).
- [4] Swanmy, R. N., & Ali, S. A. R. (1982). Punching Shear Behavior of Reinforced Slab-Column Connections Made with Steel Fiber Concrete. (1982). *ACI Journal Proceedings*, 79(5). doi:10.14359/10917.
- [5] Narayanan, R., & Darwish, I. Y. S. (1987). Punching shear tests on steel-fibre-reinforced micro-concrete slabs. *Magazine of Concrete Research*, 39(138), 42–50. doi:10.1680/mac.1987.39.138.42.
- [6] Alexander, S. D. B., & Simmonds, S. H. (1992). Punching shear tests of concrete slab-column joints containing fiber reinforcement. *ACI Structural Journal*, 89(4), 425–432. doi:10.14359/3027.
- [7] Harajli, M. H., Maalouf, D., & Khatib, H. (1995). Effect of fibers on the punching shear strength of slab-column connections. *Cement and Concrete Composites*, 17(2), 161–170. doi:10.1016/0958-9465(94)00031-S.
- [8] McHarg, P. J., Cook, W. D., Mitchell, D., & Yoon, Y. S. (2000). Benefits of concentrated slab reinforcement and steel fibers on performance of slab-column connections. *ACI Structural Journal*, 97(2), 225–234. doi:10.14359/851.
- [9] Cheng, M. Y., & Parra-Montesinos, G. J. (2010). Evaluation of steel fiber reinforcement for punching shear resistance in slab-column connections- part I: Monotonically increased load. *ACI Structural Journal*, 107(1), 101–109. doi:10.14359/51663394.
- [10] Yagoub, M., Mellas, M., Benchabane, A., & Zatar, A. (2022). Experimental Characterization of a Functionally Graded Composite Using Recycled Steel Fiber. *Civil Engineering Journal*, 8(5), 879–894. doi:10.28991/CEJ-2022-08-05-03.
- [11] Lisienkova, L., Shindina, T., Orlova, N., & Komarova, L. (2021). Optimization of the Concrete Composition Mix at the Design Stage. *Civil Engineering Journal*, 7(8), 1389–1405. doi:10.28991/cej-2021-03091732.
- [12] Singh, V., & Sangle, K. (2022). Analysis of vertically oriented coupled shear wall interconnected with coupling beams. *HighTech and Innovation Journal*, 3(2), 230–242. doi:10.28991/HIJ-2022-03-02-010.
- [13] Theodorakopoulos, D. D., & Swamy, N. (1993). Contribution of steel fibers to the strength characteristics of lightweight concrete slab-column connections failing in punching shear. *ACI Structural Journal*, 90(4), 342–355. doi:10.14359/3957.
- [14] Shaaban, A. M., & Gesund, H. (1994). Punching shear strength of steel fiber reinforced concrete flat plates. *ACI Structural Journal*, 91(4), 406–414. doi:10.14359/4145.
- [15] Mahdi, M. S., Saleh, I. S., & Faleh, S. K. (2022). Destructive and Nondestructive Tests for Concrete Containing a Various Types of Fibers. *Civil Engineering Journal*, 8(11), 2461–2475. doi:10.28991/CEJ-2022-08-11-07.
- [16] Al-Fouadi, W. K. A., Mohammed, A. H., & Abdullah, K. (2019). Experimental and analytical study on behavior of pull-out failure of reinforcing bar embedded in concrete blocks. *Structural Concrete*, 20(1), 171–184. doi:10.1002/suco.201700230.
- [17] Maya, L. F., Fernández Ruiz, M., Muttoni, A., & Foster, S. J. (2012). Punching shear strength of steel fibre reinforced concrete slabs. *Engineering Structures*, 40, 83–94. doi:10.1016/j.engstruct.2012.02.009.
- [18] Mohammed, A. H., Khalaf, R. D., Mohammedali, T. K., & Hussin, A. K. (2019). Experimental Study on Performance of Fiber Concrete-filled Tube Columns under Axial Loading. *International Journal of Engineering, Transactions B: Applications*, 32(12), 1726–1732. doi:10.5829/IJE.2019.32.12C.05.
- [19] ACI 318-11. (2011). *Building Code Requirements for Structural Concrete (ACI 318-11) and Commentary on Building Code Requirements for Structural Concrete (ACI 318R-19)*. American Concrete Institute, Michigan, United States.

- [20] Fédération Internationale du Béton (FIB). (2010). Model Code 2010 – first complete draft, vol. 1, Fédération Internationale du Béton (FIB), Bulletin 55. Lausanne, Switzerland.
- [21] Fédération Internationale du Béton (FIB). (2010). Model Code 2010 – first complete draft, vol. 2, Fédération Internationale du Béton (FIB), Bulletin 55. Lausanne, Switzerland.
- [22] JSCE. (2007). Standard specifications for concrete structures-2007, Design. Japan Society of Civil Engineers, Tokyo, Japan.
- [23] Truong, G. T., Choi, K. K., & Kim, C. S. (2022). Punching shear strength of interior concrete slab-column connections reinforced with FRP flexural and shear reinforcement. *Journal of Building Engineering*, 46(5), 409–20. doi:10.1016/j.job.2021.103692.
- [24] Higashiyama, H., Ota, A., & Mizukoshi, M. (2011). Design Equation for Punching Shear Capacity of SFRC Slabs. *International Journal of Concrete Structures and Materials*, 5(1), 35–42. doi:10.4334/ijcsm.2011.5.1.035.
- [25] Siburg, C., Hegger, J., Furche, J., & Bauermeister, U. (2014). Durchstanzbewehrung für Elementdecken nach Eurocode 2. *Beton-Und Stahlbetonbau*, 109(3), 170–181. doi:10.1002/best.201300075. (In German).
- [26] Gouveia, N. D., Faria, D. M. V., & Ramos, A. P. (2019). Assessment of SFRC flat slab punching behaviour - Part I: Monotonic vertical loading. *Magazine of Concrete Research*, 71(11), 587–598. doi:10.1680/jmacr.17.00343.